A Numerical Procedure for Aerodynamic Optimization of Helicopter Rotor Blades

J. Zibi, G. Defresne*, M. Costes

ONERA, 29 av. de la Division Leclerc, B.P. 72,
92322 Châtillon Cedex, France

Abstract

An aerodynamic optimization procedure is developed for rotor blade design, and is applied to define optimum airfoil characteristics in high speed forward flight. For that purpose, the CONMIN optimizer was coupled to a helicopter rotor performance code, R85 developed by Eurocopter France. The objective function to be minimized is the power necessary to drive the rotor, and constraints are imposed on aerodynamic and geometrical characteristics, among which the pitch–link loads are the most important. The airfoil tables for the profiles defining the blade are interpolated among a set of airfoil tables for existing or extrapolated airfoils, and the design variables are these interpolation coefficients. Numerical results show that significant improvements can be obtained on the rotor lift–to–drag ratio by thinning the blade, the rotor performance at high lift being recovered by cambering the airfoils.

1 Introduction

The design of helicopter rotor blades requires a large number of calculations through a systematic parametric study, in which the large number of blade definition parameters are varied in an analytical rotor model, in order to meet the project requirements. The increasing complexity of rotors, as well as the enlarging helicopter flight envelope, in particular at high speeds, calls for more and more human resources and CPU time in practical design.

An efficient way to fulfill these requirements can be obtained by using optimization techniques, capable of repeating tasks automatically and finding the best compromise solution to the design problem with reduced manpower. Indeed, this kind of process has overcome inverse design problems for airfoils, [1][2], and allowed to improve significantly airfoil characteristics, e.g. for helicopters. For three–dimensional aerodynamic configurations, numerical optimization is not so advanced because aerodynamic calculations are very computer–time consuming, and therefore cannot be integrated easily in an optimization process. Only first applications to fixed wing design begin to be performed with 3D CFD techniques coupled to a numerical optimizer [3].

As far as helicopter rotors are concerned, the particular flow characteristics make the calculation so difficult that such a procedure will not be possible within the next few years. As a matter of fact, the flow is so complex that no full rotor calculation can be expected in the near future. One can mention the flow unsteadiness, the transonic conditions on the advancing blade side, subsonic

* Presently at SEDITEC, 17 Avenue Didier Daurat, 31700 Blagnac, FRANCE.

and highly viscous characteristics on the retreating blade. Furthermore, the blade motion and deformation are linked to the flight conditions, and therefore have to be solved simultaneously with the aerodynamic equations. This is the reason why, presently, optimization techniques for blade design use simpler rotor analysis, which are typically industry tools for design. They have simple aerodynamic models, using the lifting line theory and experimental 2D airfoil tables, but more refined dynamic models, which use beam theory with either a modal approach or finite-element methods [4]. Since numerical optimization implies a reliable estimate of design variables gradients, the first applications to rotor blades concerned rotor dynamics. The necessity to improve rotor aerodynamics has led to the use of these relatively simple models for aerodynamic optimization. Nevertheless, such aerodynamic models have been improved and validated through wind tunnel tests, in order to model advanced non rectangular rotor blades. NASA and the US-Army have a well-known multidisciplinary programme on this topic [5]. In France, ONERA and Eurocopter, with the financial support of the French Ministry of Defense, STPA and DRET, have a joint programme on rotor aerodynamic and dynamic optimization, called ORPHEE. An example of the aerodynamic design performed at ONERA in this framework is presented below. It deals with the determination of optimum airfoil characteristics for high speed forward flight, using interpolations on lift, drag and pitching moment curves.

2 Optimization methodology

2.1 Description of the CONMIN algorithm

The CONMIN optimizer [6] is based on the feasible directions theory. It consists in minimizing an objective function inside an admissible domain, defined by constraints. These constraints concern either the design variables themselves or non-optimized variables. In the case of design variables, these constraints, called "side constraints", correspond to the lower and upper bounds of each design variable and determine the domain of validity of the optimization variables. The surface where a constraint G is equal to zero separates the space in two zones, and the zone where G is negative is the feasible region. The optimization domain represents the intersection of all these "half-spaces".

The optimization algorithm consists in calculating, for a given iteration, the "best" search direction, along which the objective function is most decreasing without violating any constraint. A typical iteration for this optimization procedure can be described as follows :

- for a given initial state X^n, the objective function derivatives with respect to each decision variable are calculated in CONMIN by finite differences with a typical step equal to one percent of the value of the decision variable ;

- once the gradient vector of the objective function is known at X^n, the search direction is calculated by a modified conjugate gradient method which allows to stay in the admissible domain by calculating the gradients of the active constraints along the domain boundaries ;

– then, the advancing step, which determines how far the design variable X^n will be moved in the design space to minimize the objective function without violating any constraint, is calculated using one dimensional optimization. In general, three iterations are necessary to define the new state X^{n+1}.

2.2 Description of the R85 rotor performance code

This code was developped at ECF to provide a versatile and efficient tool able to compute the rotor performance for analysis and design [7]. A flowchart of the code is shown in figure 1. The rotor is trimmed by iteratively solving mechanical equations written for the rotor blades to which aerodynamic and inertial stresses are applied.

The blade aerodynamics is simulated using a simple quasi–steady lifting line analysis, for which blade sections are taken into account with 2D airfoil tables. The wake effect is included either with a simple Meijer–Drees inflow model or with a vortex wake of prescribed geometry (called METAR). Several model refinements can be applied to simulate non rectangular blades.

The dynamics blade model includes either a rigid blade or a flexible blade simulation. In the flexible formulation, it solves the non linear Lagrange equations, using a modal decomposition of the blade. A hub description, as well as the local blade section mass, stiffness and inertia are a necessary input.

The rotor trim can be obtained for various types of conditions. These can be either prescribed loads, prescribed input controls or a combination of the two.

2.3 Coupling CONMIN/R85

The CONMIN optimizer is coupled with the aeroelastic rotor code, R85. The rotor optimization flowchart is presented in figure 2. For given rotor geometry and flight condition, the R85 code gives the pitch, flag and lag angles as well as the rotor loads and power provided to the rotor. These values are transmitted to the optimization subroutine through the objective function and constraints. If N is the number of decision variables, an iteration requires in general (N+3) objective function calculations, ie the loop described in figure 2 is performed (N+3) times. This shows why the rotor modeling program has to be fast enough to minimize CPU times. The METAR wake model is more realistic than the Meijer–Drees one, but needs more CPU time, and therefore only the Meijer–Drees inflow model is used during the optimization procedure.

For the present case, the objective is to minimize the power consumed by the main rotor in high speed forward flight, more precisely at the point (V=350km/h, C_L/σ=0.075). The constraints vector is defined by aerodynamic and geometrical requirements. Among them, the pitch link loads which are the limiting factor on the control system, are the most important. The selected variables are the twist angle, chord distribution, airfoil polars and airfoil positions along the blade.

3 Definition of optimized airfoil polars

An original application of this optimization procedure will be described in this section to illustrate its capabilities. It concerns the definition of optimized airfoil polars for a rotor in high speed forward flight.

3.1 Interpolation of airfoil polars

A blade is defined by at most five different airfoils, each of them being interpolated between at most five polars. The design variables are the interpolation coefficients λ. Constraints relative to these variables are defined as follows :

* $0 \leq \lambda_{ij} \leq 1$, i=1,..,n and j=1,..,m(n)

with n being the number of airfoils along the blade (≤ 5)

m(i) being the number of polars defining the i^{th} airfoil (≤ 5)

* $\sum_{i=1}^{n} \lambda_{ij} = 1$, j=1,..,m(n)

The last m constraints are implicitly imposed by the following relation :

$$\lambda_{nj} = 1 - \sum_{i=1}^{n-1} \lambda_{ij} \ , \ j=1,..,m(n)$$

So, one has : $0 \leq \lambda_{nj} = 1 - \sum_{i=1}^{n-1} \lambda_{ij} \leq 1$, so $0 \leq \sum_{i=1}^{n-1} \lambda_{ij} \leq 1$, j=1,..m(n)

Therefore, there are (m(i)−1) optimization variables left in each polar−section defining the blade.

During the optimization process, airfoil polars are interpolated in a polar file, made of existing or extrapolated airfoils. These extrapolated airfoils concern non zero moment coefficient airfoils since few data is available for this type of airfoils for helicopters. The basic idea is, as was done for the BERP blade [8], to relax constraints on low moment coefficients to allow larger lifting capabilities while maintening moderate pitch link loads for the whole rotor by a global balance all along the blade span. It is well known that a lower moment coefficient (nose−down) allows a higher lift capability as shown in the figure 3. An empirical rule for this gain of lift was defined by compiling existing data.

This empirical correction was applied to existing helicopter airfoils which were used in the optimization process. In order to get rid of reference problems and be able to compare polars, the angles of incidence were shifted so that zero lift corresponds to zero incidence.

3.2 Optimized airfoils results

The optimization process has been initialized by a four−bladed rotor reference. Blades are rectangular and airfoils are OA312, from 20 to 85% radius, and OA309 from 92% radius to the tip (figure 4). The rotor issued from

this optimization process has three definition airfoils, but only two of them are optimized. As a matter of fact, the accuracy of the rotor code is not sufficient at the blade tip for optimization purpose. This explains why no airfoil is optimized at the blade tip and the OA309 airfoil is kept for the last 5% of the radius.

The optimized rotor has the following airfoils distribution :

– from 20 to 54% radius, the inner airfoil, whose relative thickness is equal to 11%, has a nose–up pitching moment coefficient (Cm0=0.044) ;

– from 59 to 89% radius, the intermediate airfoil, whose relative thickness is equal to 9%, has a nose–down pitching moment coefficient (Cm0=–0.020) ;

– from 92% radius to the tip, the OA309 airfoil is used (Cm0=0.002).

In its median part, the optimized blade has a lower relative thickness than the reference blade.

Around the optimization point (μ=0.45, C_L/σ=0.075), a benefit on the consumed power, equal to 4.3% is obtained by the optimized rotor (with respect to the baseline rotor). The optimized rotor performance is improved in the overall flight domain, except at high lifts where stall occurs earlier. A parametric study shows that power gains are increasing with the advance ratio parameters (figure 5). The hover performance of the optimized rotor is also slightly better than the reference rotor (figure 6).

Figure 7 shows the computed pitch link loads for the optimized and the reference rotors. Thanks to the constraints vector, the optimized airfoil distribution allows to decrease these loads relatively to the reference rotor.

This survey shows that a one–point optimization procedure is sufficient to obtain power benefits in all the flight domain. This is due essentially due to appropriate choices of initialisation variables between each successive iteration during the optimization process.

4 Results analysis

To explain more precisely the origin of power benefits, three rotors will be compared :

– the baseline rotor ;

– an intermediate rotor, for which only positions of the OA312 and OA309 airfoils are optimized along the span, in order to separate the different effects (airfoil curves, relative thickness decreasing) ;

– the optimized rotor.

First of all, figure 8 shows a comparison between the optimized rotor intermediate airfoil, the OA312 and the OA309 polars curves. The lift capabilty is improved for the optimized airfoil at transonic speed without increasing the drag, thus giving a higher lift–to–drag ratio. At low speed, this 9% thick airfoil has a maximum lift capability close to that of the OA312.

The drag azimuthal evolution, at 89% radius (corresponding to the upper bound of the intermediate airfoil of the optimized rotor), at the optimization point, shows differences between the three rotors (figure 9). The decrease of the

relative thickness value of the optimized rotor can explain the drag reduction, especially in the advancing side ($0°<\Psi<180°$). On the other hand, lift is similar for the three rotors (figure 10), showing that significant benefits are obtained on the rotor lift–to–drag ratio. Therefore, the rotor performance is improved at high speed and moderate lift conditions, by thinning the blade.

For a flight configuration closer to stall ($C_L/\sigma=0.09$), the spanwise loads evolution for $\psi=300°$ (figures 11 and 12), shows the major role of the intermediate airfoil of the optimized rotor. This airfoil avoids the local stall by its negative moment coefficient, increasing then its lifting capabilities, whereas flow separation probably occurs on the OA309 airfoil at the corresponding part of the intermediate rotor. The maximum lift loss brought by thinning the blade is recovered by cambering the intermediate airfoil on the optimized blade, giving it lift performances close to those of the OA312 airfoil.

5 Future evolutions

During the optimization process described above, only the Meijer–Drees inflow model has been used. This model has the advantages to be simple, robust and to have low cost in CPU time. But, it does not take into account the wake interactions. It would be interesting to introduce the METAR model during the first optimization iteration, in order to have a better initialisation of the induced velocities, as well as a better prediction of the load distribution at the tip.

On the other hand, blades were supposed to be rigid. The degrees of freedom are the rigid motions of the blades around the flap, pitch and lag hinges. It would be of interest to improve the dynamic model by introducing the R85 flexible blade model. In this case, loads applied to the rotor blades are calculated by taking into account the blades bendings.

Finally, a one–point optimization process has allowed to define optimum airfoil characteristics for a rotor in high speed forward flight. Performance has been improved for the optimization point but also in all the flight domain. It would be interesting to introduce a multi–point optimization procedure, in order to avoid the possibility of finding a local optimum design. Though this optimization process is longer than for a one point optimization, it would allow to find a good compromise between several points.

6 Conclusion

Two new airfoils for rectangular–bladed rotors in high speed forward flight have been designed. The optimized rotor is defined as follows :

– the inner airfoil (11% of relative thickness) has an important nose–up pitching moment coefficient ;

– the intermediate airfoil (9% of relative thickness) has a moderate nose–down pitching moment coefficient. It allows to compensate control loads introduced by the inner airfoil, and to improve the maximal lift coefficient ;

– the outer airfoil is OA309.

At the optimization point (V=350km/h, C_L/σ=0.075), power benefits are greater than 4% with respect to the baseline rotor. These gains are essentially due to the relative thinning of the optimized rotor. Results issued from this one-point optimization process show that the optimized rotor has better performance than the reference rotor in the overall flight domain.

From the specifications given by the present optimization procedure, new airfoils were designed. They will equip a new rotor which will be tested in the ONERA S1MA wind tunnel to validate this work.

References

[1] J. Reneaux and J.J. Thibert, The Use of Numerical Optimization for Airfoil Design, AIAA 3th Applied Aerodynamics Conference, Colorado Springs, Colorado (USA), October 1985.

[2] H. Bézard, Rotor Blade Airfoil Design by Numerical Optimization and Unsteady Calculations, 48th AHS Forum, Washington D.C., June 1992.

[3] D. Destarac, D. Reneaux and D. Gisquet, Numerical Optimization of Wings in Transonic Flow, AGARD Conference, Norway, May 1989.

[4] J.W. Lim and I. Chopra, Aeroelastic Optimization of a Helicopter Rotor, 44th AHS Forum, Washington D.C., June 1988.

[5] H.M. Adelman, W.R. Mantay, J.L. Walsh and J.I. Pritchard, Integrated Multidisciplinary Rotorcraft Optimization Research at the NASA Langley Research Center, Vertiflite, March-April 1992, Vol38, No2.

[6] G.N. Vanderplaats, CONMIN - A Fortran Program for Constrained Function Minimization, NASA TMX 62,282, 1973.

[7] M. Allongue and T. Krysinsky, Validation of a New General Aerospatiale Aeroelastic Rotor Model Through the Wind Tunnel and Flight Tests Data, 46th AHS Forum, Washington D.C. May 1990.

[8] F.J. Perry, Aerodynamics of the Helicopter World Speed Record, 43rd AHS Forum, St Louis Missouri, May 1987.

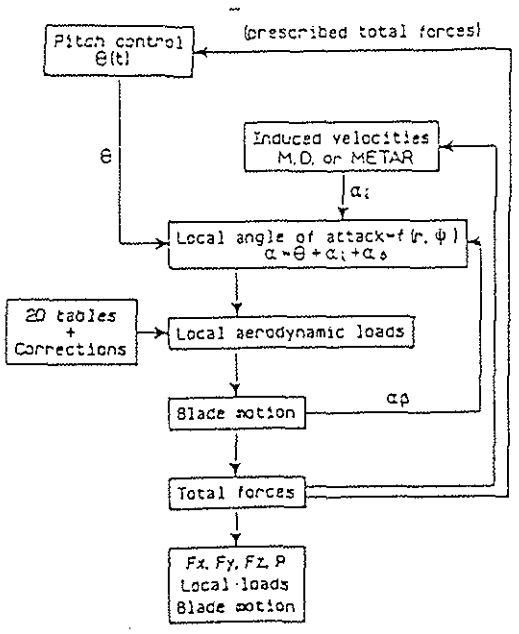

Fig. 1 - R85 flowchart.

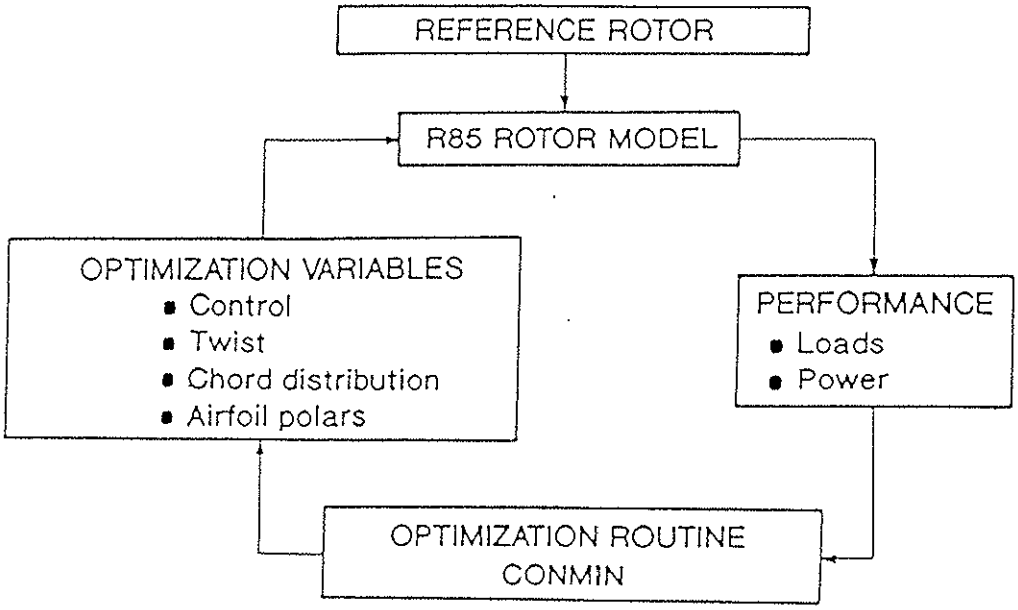

Fig. 2 - Rotor optimization chart.

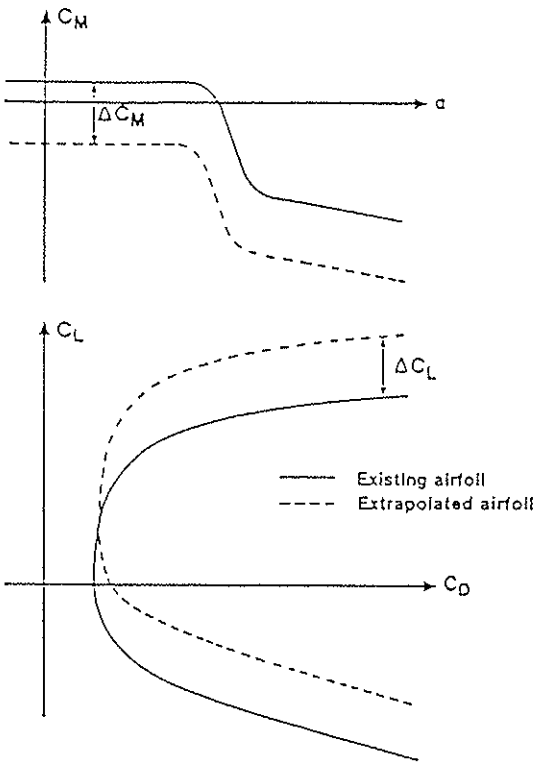

Fig. 3 - Definition of extrapolated airfoil polars.

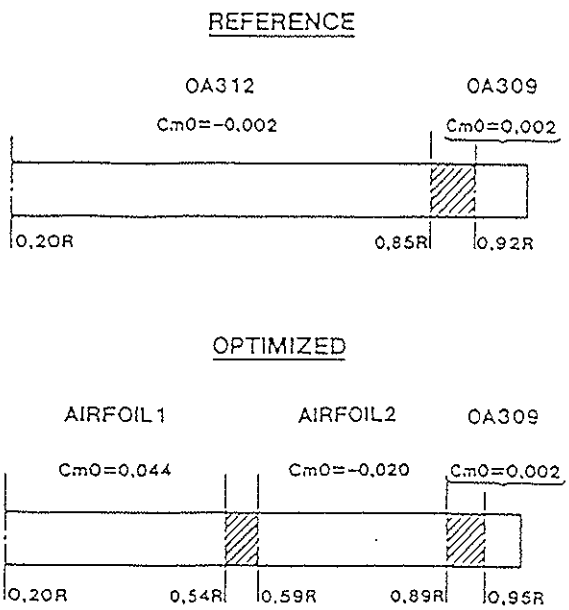

Fig. 4 - Airfoil optimization for high speed flight.

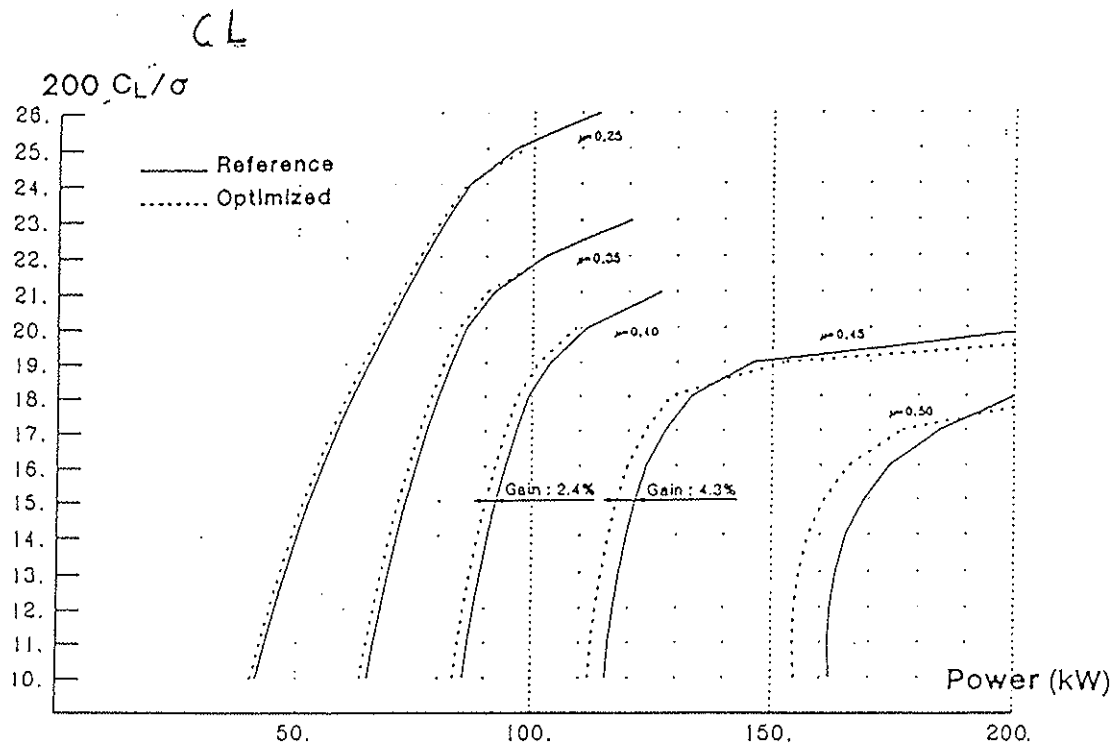

Fig. 5 - Flight envelope.

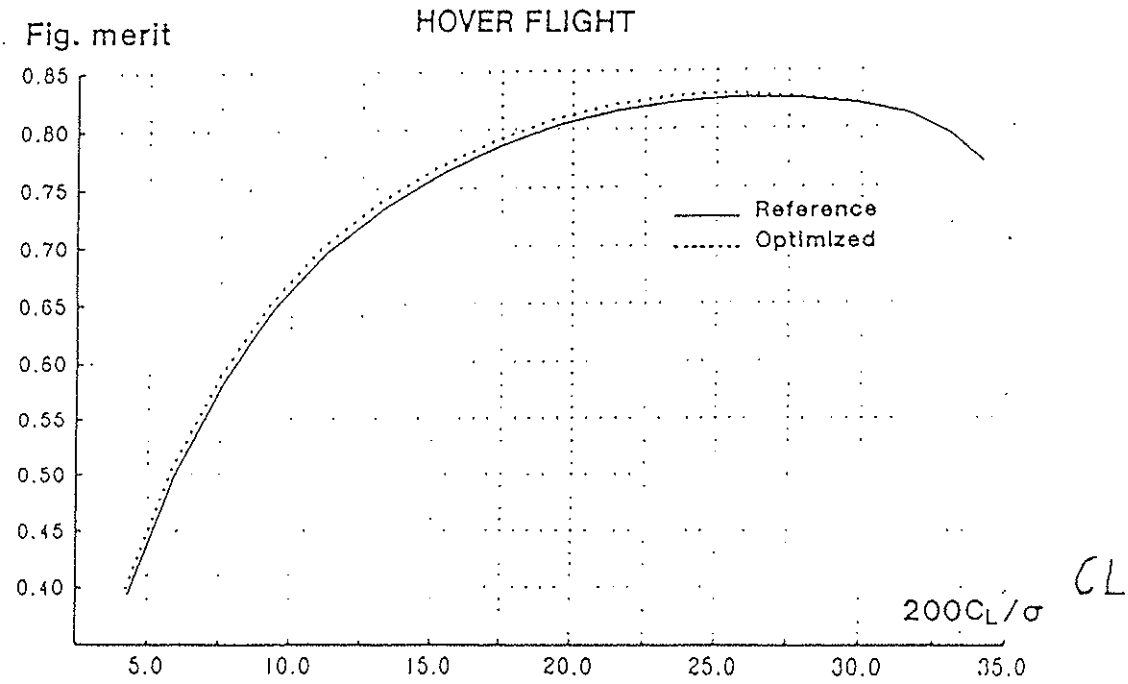

Fig. 6 - Rotor comparison.

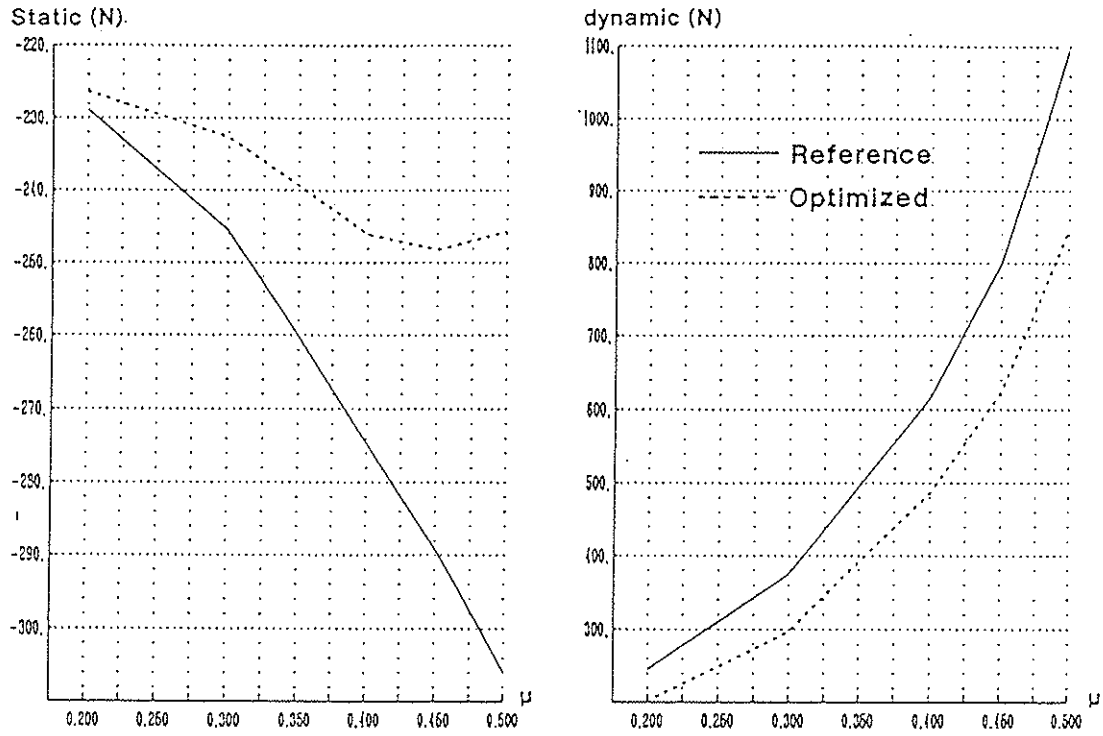

Fig. 7 - Rotor comparison pitch link loads.

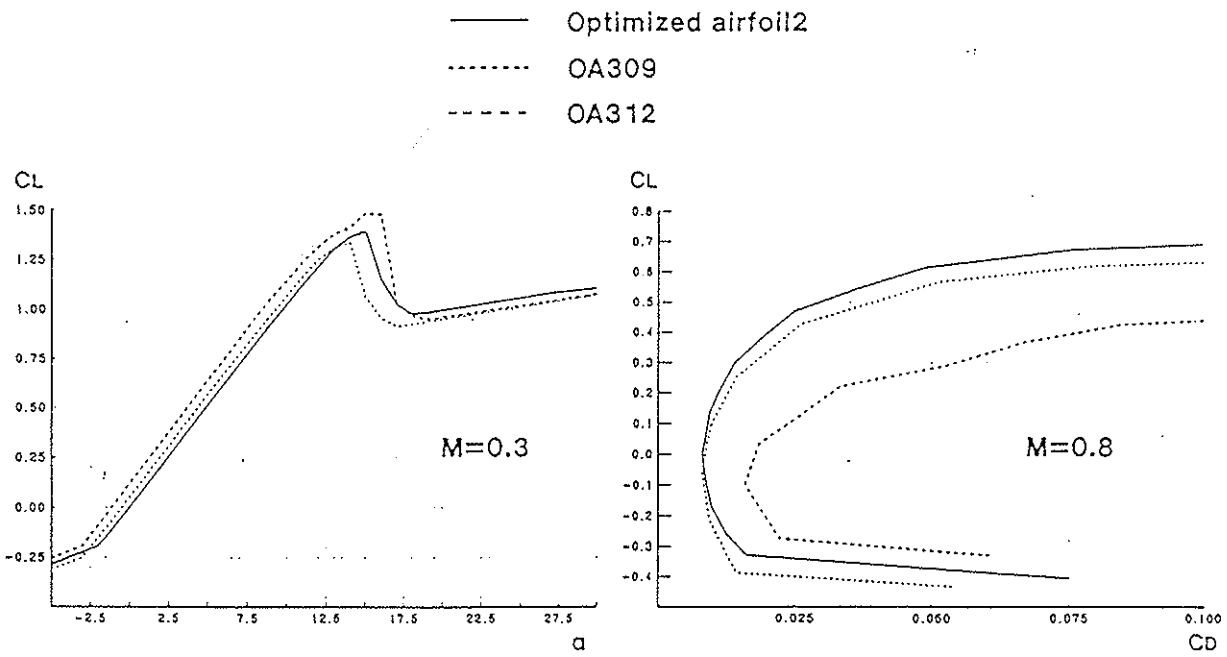

Fig. 8 - Airfoil comparison .

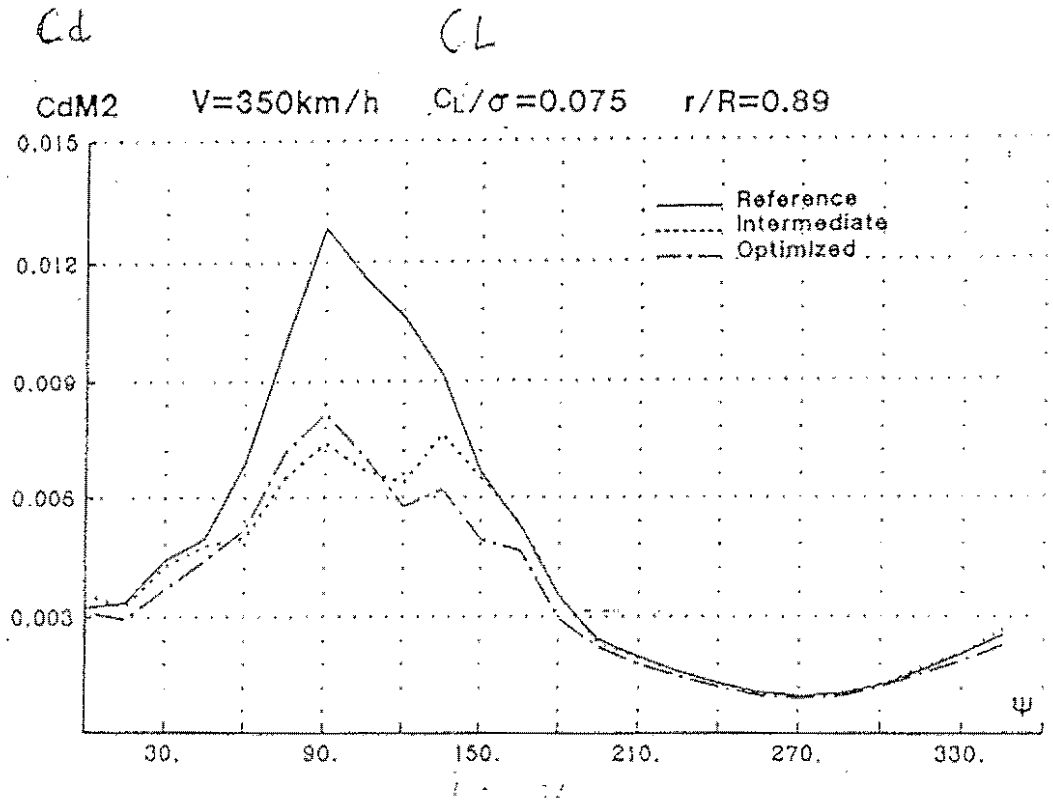

Fig. 9 - Rotor comparison.

9

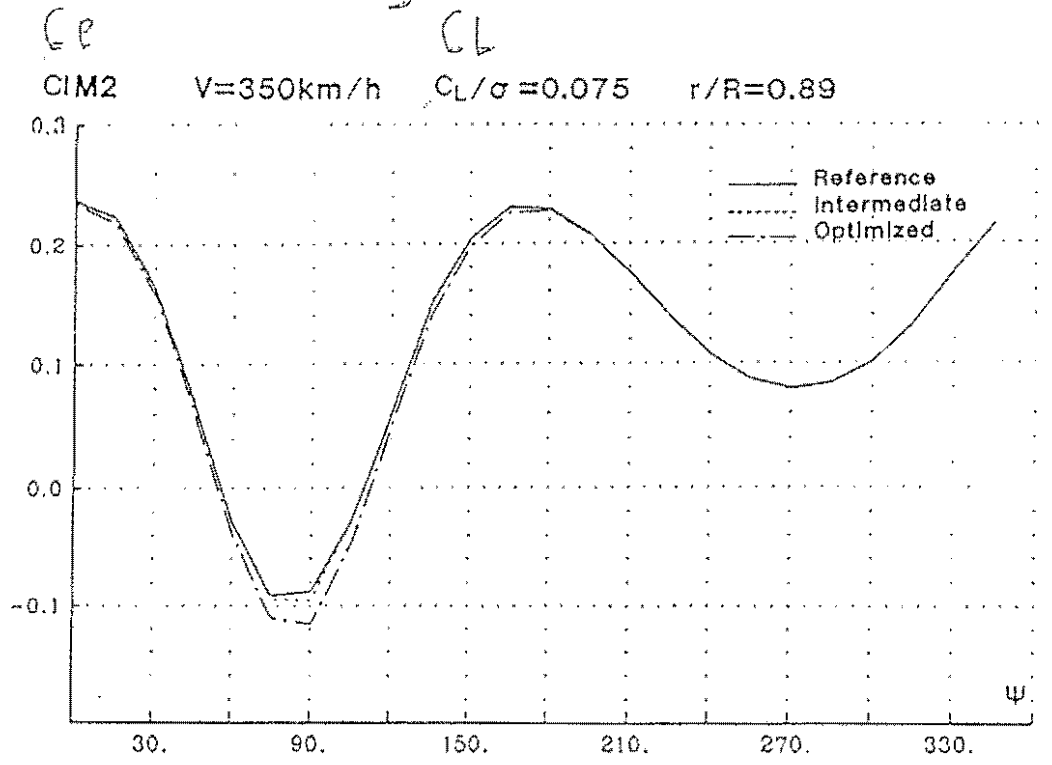

Fig. 10 - Rotor comparison.

10

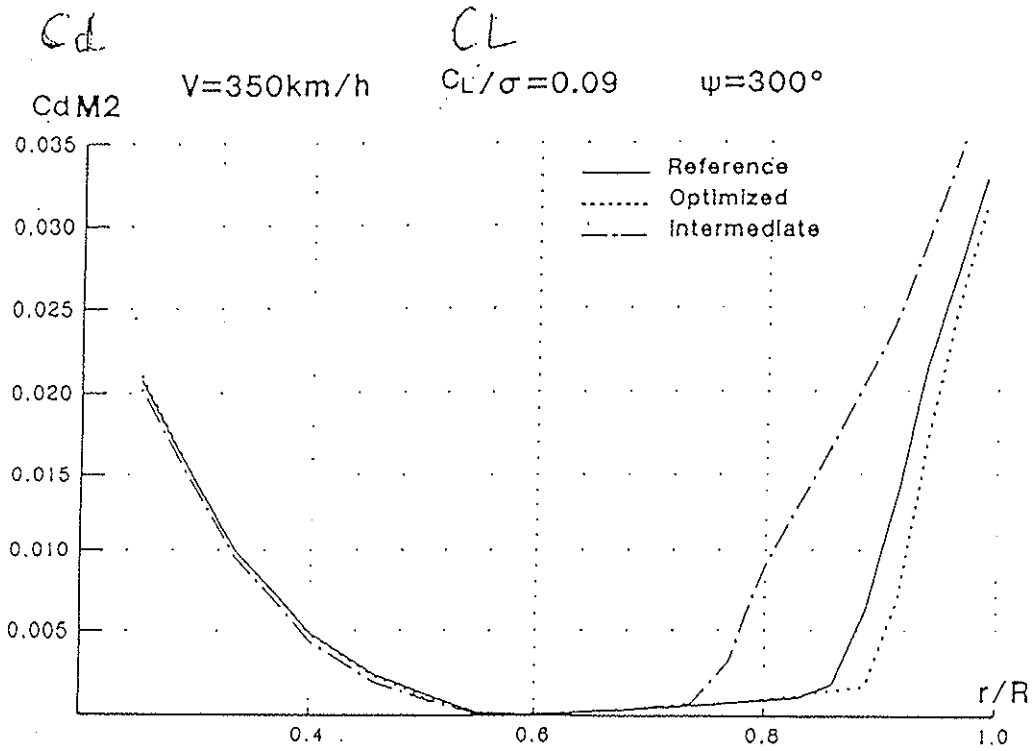

Fig. 11 - Rotor comparison.

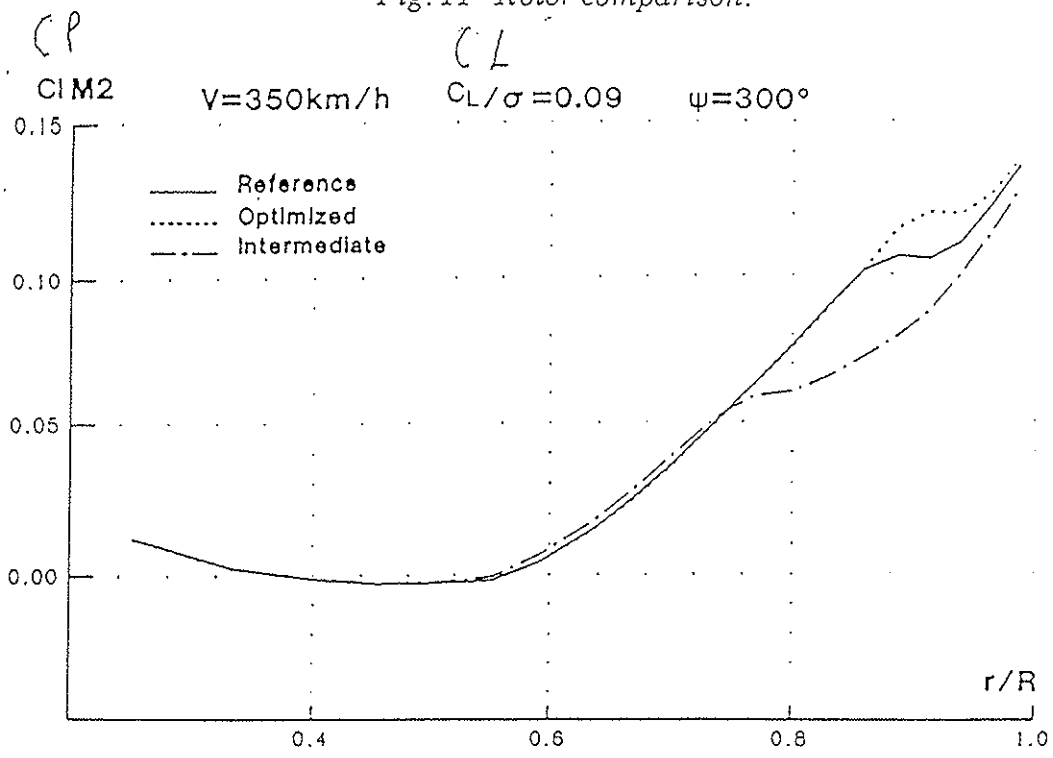

Fig. 12 - Rotor comparison.

12